ACTIVE NOISE CONTROL USING THE PERTURBATION METHOD —VERIFICATION IN ACTUAL MULTI-CHANNEL SYSTEMS–

Tasuku Ainoya, Takashi Mori, Yoshinobu Kajikawa and Yasuo Nomura

Department of electronics, Faculty of Engineering, Kansai University
t.ainoya,kaji@joho.densi.kansai-u.ac.jp

ABSTRACT

In this papar, we verify effectiveness of multi-channel active noise control (ANC) systems using the perturbation method in actual systems. The multi-channel perturbation method has an advantage that secondary path models (estimation of secondary paths) are unnecessary compared with the MEFXLMS method applying the Filtered-x LMS method to multi-channel systems. The multi-channel ANC systems using the perturbation method will be cosequently able to control noise stably because these do not have modeling errors which cause system instability. We therefore verify that the multi-channel ANC systems using the perturbation method can operate stably in the enviroment that the secondary paths always change.

1. PERTURBATION METHOD

The perturbation method is an algorithm that calculates an estimation of gradient vector by adding a little perturbation to the coefficient of noise control filter. The perturbation method is classified into several algorithms. In this paper, the time domain time difference simultaneous perturbation (TDTDSP) method [1] and the frequency domain time difference simultaneous perturbation (FDTDSP) method [2] are explained as follows.

1.1. TDTDSP method

The TDTDSP method is an algorithm which updates the filter coefficients once every N samples by using only one kind of error signal. The perturbation is always added to the coefficients of the noise control filter, and the error signals with the perturbation is obtained in the block period N. The filter coefficients at the nth block are updated using the average values of two error signals obtained in the nth and $n-1$th block periods.

The updating algorithm at the nth block based on above idea is defined as follows:

$$\mathbf{w}_{n+1} = \mathbf{w}_n - \mu\Delta\mathbf{w}_n \tag{1}$$

$$\Delta\mathbf{w}_n = \frac{e_n - e_{n-1}}{(c_n\mathbf{s}_n - c_{n-1}\mathbf{s}_{n-1} - \mu\Delta\mathbf{w}_{n-1})N} \tag{2}$$

$$e_n = \sum_{k=nN+1}^{(n+1)N} J(\mathbf{w}_n + c_n\mathbf{s}_n) \tag{3}$$

We use a diagram to explain the above equation. Figure 1 shows an error-performance surface, which shows the relation between the ith filter coefficient $w(i)$ and the square error $J(\cdot) = e_k^2$. It can be seen from Fig. 1 that an estimation of the gradient vector is obtained by dividing a difference of $J(w_n(i) + c_n s_n(i))$

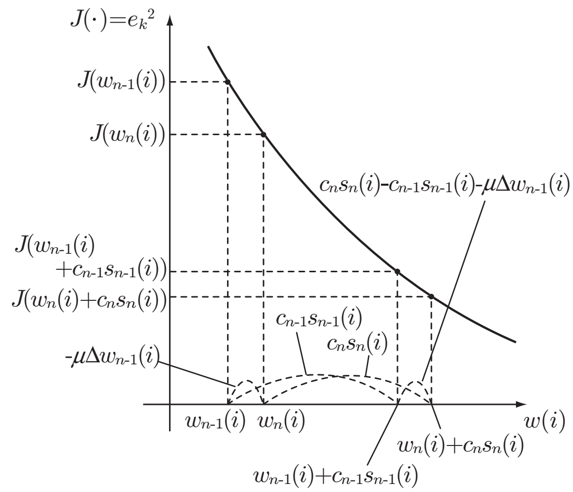

Fig. 1. Error-performance surface at the ith filter coefficient $w(i)$.

and $J(w_{n-1}(i) + c_{n-1}s_{n-1}(i))$ by $c_n s_n(i) - c_{n-1}s_{n-1}(i) - \mu\Delta w_{n-1}(i)$.

By the way, we cannot in fact calculate the exact estimation of the gradient vector by using Eq.(2). Because the error-performance surface shown in Fig. 1 changes while obtaining the error signals which are used to calculate the factors $J(w_n(i)+c_n s_n(i))$ and $J(w_{n-1}(i)+c_{n-1}s_{n-1}(i))$. That is, an error occurs due to obtaining these factors at different times. If the denominator of Eq.(2) becomes small, then the ANC system may become unstable due to the increase of this error. In order to avoid this problem, Eq.(2) is modified as follows:

$$\Delta\mathbf{w}_n = \frac{e_n - e_{n-1}}{c_n N}\mathbf{s}_n \tag{4}$$

In the case of using Eq.(4), the above problem can be avoided. However, a new error occurs in the denominator of Eq.(4) due to the omission of the terms of $c_{n-1}\mathbf{s}_{n-1}$ and $\mu\Delta\mathbf{w}_{n-1}$ of Eq.(2). This error does not influence a convergent value of the filter coefficients because it does not correlate with $\mathbf{s}_n$. But it does influence the instantaneous correction value of the filter coefficients, such as measurement noise. The influence of $\mu\Delta\mathbf{w}_n$ can be ignored because it is too smaller than $c_{n-1}\mathbf{s}_{n-1}$. Moreover, the influence of $c_{n-1}\mathbf{s}_{n-1}$ depends on the magnitude of the perturbation. Therefore, the influence becomes small as c_n becomes small. The TDTDSP method consequently becomes effective.

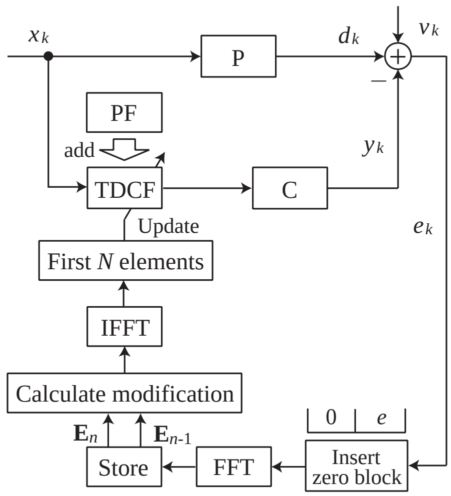

Fig. 2. Block diagram of the ANC system using the frequency domain time difference simultaneous perturbation method.

1.2. FDTDSP method

The ANC system using the FDTDSP method is shown in Fig. 2. In this system, the filtering operation is done in the time domain and the updating operation is done in the frequency domain, in order that the ANC system must reduce noise in real time. The FDTDSP method can converge faster than the TDTDSP method because the coefficients of the noise control filter is updated in the frequency domain [3]. The updating algorithm at the nth block is defined as follows:

$$\mathbf{w}_{n+1} = \mathbf{w}_n - \mu \Delta \mathbf{w}_n \tag{5}$$

$$\Delta \mathbf{w}_n = \text{first } N \text{ elements of IFFT}[\mathbf{U}_n] \tag{6}$$

$$\mathbf{U}_n = \text{diag}[\mathbf{S}_n] \frac{\text{diag}[\mathbf{E}_n^*]\mathbf{E}_n - \text{diag}[\mathbf{E}_{n-1}^*]\mathbf{E}_{n-1}}{c_n} \tag{7}$$

$$\mathbf{E}_n = \text{FFT}[0 \cdots 0 \; e_{nN+1} \cdots e_k \cdots e_{(n+1)N}]^T$$

$$\mathbf{S}_n = [S_n(1) \; S_n(2) \cdots S_n(i) \cdots S_n(2N)]^T$$

where $\mathbf{S}_n$ is a complex vector whose elements are -1 or 1 in both real and imaginary parts and has the following characteristics:

$$\begin{aligned}
&E[\text{Re}\{S_n(i)\}] = 0, \; E[\text{Im}\{S_n(i)\}] = 0 \\
&\text{Re}\{S_n(i)\}^2 = 1, \; \text{Im}\{S_n(i)\}^2 = 1 \\
&E[\text{Re}\{S_n(i)\}\text{Re}\{S_m(i)\}] = 0, \; n \neq m \\
&E[\text{Im}\{S_n(i)\}\text{Im}\{S_m(i)\}] = 0, \; n \neq m \\
&E[\text{Re}\{S_n(i)\}\text{Re}\{S_n(j)\}] = 0, \; i \neq j \\
&E[\text{Im}\{S_n(i)\}\text{Im}\{S_n(j)\}] = 0, \; i \neq j \\
&E[\text{Re}\{S_n(i)\}\text{Im}\{S_n(j)\}] = 0
\end{aligned} \tag{8}$$

1.3. Multi-channel perturbation method

In this paper, the updating algorithm in the experiment is the multi-channel FDTDSP method applying the FDTDSP method to multi-channel systems. Multi-channel ANC systems with J reference microphones, K secondary sources, and M error microphones are defined as CASE(J,K,M).

The updating algorithm at CASE(J,K,M) is defined as follows:

$$\begin{aligned}
\mathbf{w}_{lj,n+1} &= \mathbf{w}_{lj,n} - \mu \Delta \mathbf{w}_{lj,n} \\
\Delta \mathbf{w}_{lj,n} &= \text{first } N \text{ elements of IFFT}[\mathbf{U}_{lj,n}] \\
\mathbf{U}_{lj,n} &= \text{diag}[\mathbf{S}_{lj,n}] \sum_{m=1}^{M} \big\{ \text{diag}[\mathbf{E}_{m,n}^*]\mathbf{E}_{m,n} \\
&\qquad - \text{diag}[\mathbf{E}_{m,n-1}^*]\mathbf{E}_{m,n-1} \big\} / c_n \\
\mathbf{E}_{m,n} &= \text{FFT}[0 \cdots 0 \; e_{m,nN+1} \cdots e_{m,k} \cdots e_{m,(n+1)N}]^T \\
\mathbf{w}_{lj,n} &= [w_{lj,n}(1) \; w_{lj,n}(2) \cdots w_{lj,n}(i) \cdots w_{lj,n}(N)]^T \\
\mathbf{S}_{lj,n} &= [S_{lj,n}(1) \; S_{lj,n}(2) \cdots S_{lj,n}(i) \cdots S_{lj,n}(2N)]^T
\end{aligned} \tag{9}$$

where $\mathbf{w}_{lj,n}$ is the coefficient vector of the noise control filter, $\mathbf{S}_{lj,n}$ the frequency domain time simultaneous perturbation vector, n the block time, μ the step-size parameter, and c_n the magnitude of the perturbation. Moreover, c_n and $\mathbf{s}_{lj,n}$ are respectively defined as follows:

$$c_n = \sqrt{\frac{\alpha J \sum_{m=1}^{M} \sum_{k=(n-1)N+1}^{nN} e_{m,k}^2}{G^2 M \sum_{j=1}^{J} \sum_{k=(n-1)N+1}^{nN} x_{j,k}^2}} \tag{10}$$

$$\mathbf{s}_{lj,n} = \text{first } N \text{ elements of IFFT}[\mathbf{S}_{lj,n}] \tag{11}$$

where G is the mean gain of all secondary paths and α is a coefficient that defines a ratio of the power of the perturbation to the error signal.

2. MULTI-CHANNEL ANC SYSTEMS

Figure 3 shows a multi-channel ANC system using in the experiment. **Figure 4** shows block diagrams implemented in DSP for the MEFXLMS algorithm and the perturbation method, respectively. The block diagrams shown in **Fig. 3 , 4** are multi-channel ANC systems at CASE(1,2,2).

In **Fig. 4**, W_{lj} is a noise control filter in the feedforward channel from jth reference microphone to lth secondary source and $\hat{\mathrm{C}}_{ml}$ is the secondary path model estimating the secondary path from lth secondary source to mth error microphone. It can be seen from **Fig. 4** that in the realization of the ANC systems, the DSP executes the filtering and the updating. The real-time processing of the perturbation method can be easily realized compared with the MEFXLMS method. The perturbation method need not execute the filtering of the secondary path models because the perturbation method need not use the seconodary path models. Hence, in the perturbation method, the complexity in a sampling period is so small compared with the MEFXLMS algorithm. Also, the difference of the complexity for each algorithm becomes larger as the number of channels increases.

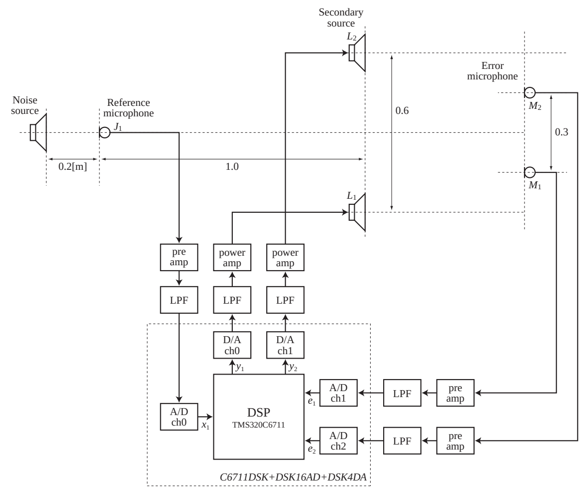

Fig. 3. Measurement model of the multi-channel ANC system.

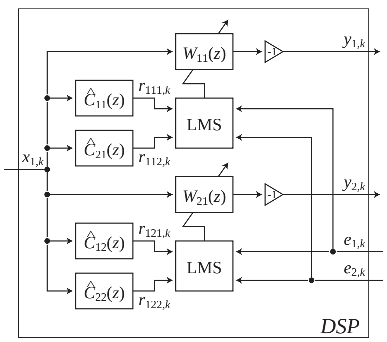

(a) MEFXLMS algorithm

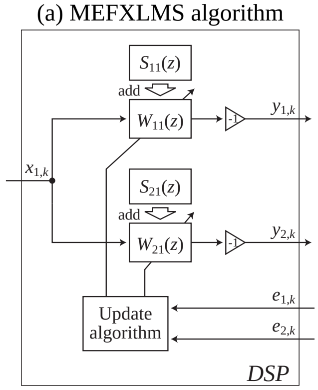

(b) Multiple-channel Perturbation method

Fig. 4. Block diagrams of the algorithm implemented in DSP.

3. EXPERIMENT

We verify the effectiveness of the ANC systems using the multi-channel perturbation method. Measurement conditions are shown in **Table 1**. The noise source is multi-sinusoidal waves (100, 130, 180, 240, 320[Hz]). In the perturbation method, α is 0.02 and G is 0.1. The arrangement in the experiment is shown in **Fig. 3**.

Table 1. Measurement conditions.

Sampling frequency	5[kHz]
Tap length of noise control filters	
MEFXLMS algorithm	80
Multiple-channel Perturbation method	128
Tap length of secondary path models	50
Cut-off frequency of anti-aliasing filter	1.56[kHz]

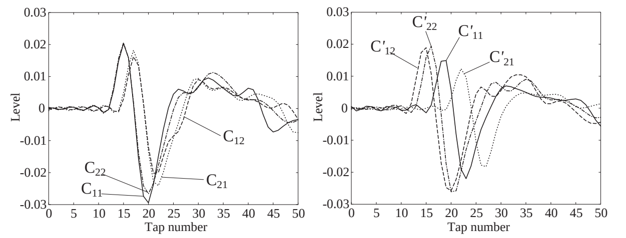

(a) before (b)after

Fig. 5. Error signals of the ANC system to multi–sinusoidal waves.

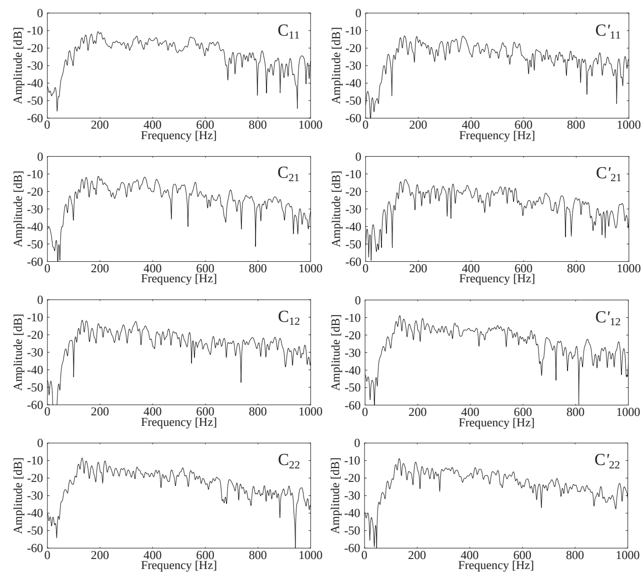

(a) before (b)after

Fig. 6. Error signals of the ANC system to multi–sinusoidal waves.

3.1. Cancellation performance

We verify the cancellation performance in the perturbation method compared with the MEFXLMS algorithm. After the ANC systems operate, the secondary paths are changed at 120 seconds. **Figure 5 , 6** show the impulse responses and frequency responses of the secondary paths before and after the secondary paths change, respectively.

Figure 7 shows error signals of the ANC system obtained in the error microphone 1. In **Fig. 7**, (a) is the case that the ANC system is stopped, (b) and (c) are the cases that the ANC system using the MEFXLMS algorithm which the step-size-parameter is 0.7 or

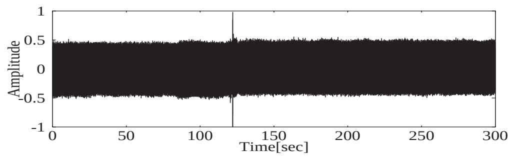

(a) Without control

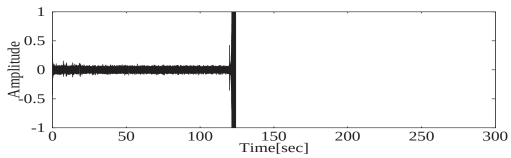

(b) With control by the MEFXLMS algorithm ($\mu = 0.7$)

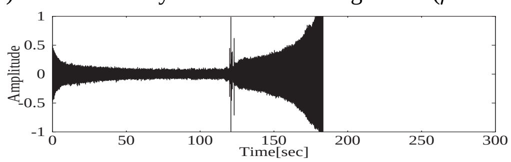

(c) With control by the MEFXLMS algorithm ($\mu = 0.007$)

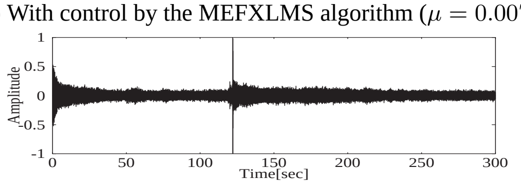

(d) With control by the perturbation method

Fig. 7. Error signals of the ANC system to multi–sinusoidal waves.

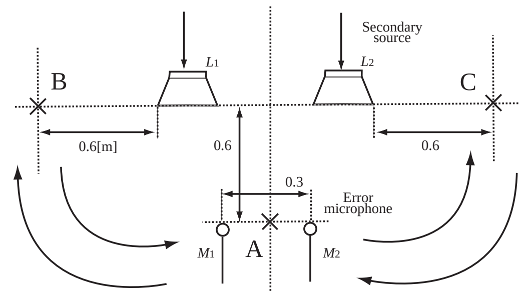

Fig. 8. Position of secondary sources and error microphones.

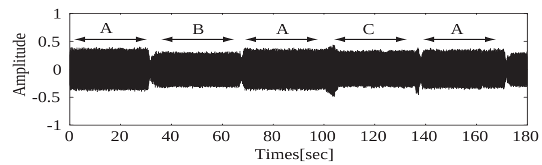

(a) Without control

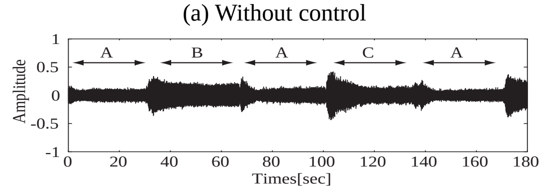

(b) With control

Fig. 9. Error signals of the ANC system to multi–sinusoidal waves.

0.007 is executed, and (d) is the case that the ANC system using the multi-channel perturbation method is executed, respectively.

It can be seen form **Fig. 7** that the perturbation method can re-converge after the secondary paths change. On the other hand, the MEFXLMS algorithm cannot re-converge, though the MEFXLMS algorithm converge faster than the perturbation method. Even if the step-size-parameter is set to too small, the ANC systems using the MEFXLMS algorithm cannot re-converge. Therefore, the ANC systems using the multi-channel perturbation method has an advantage that can operate stably in the environment which secondary paths change.

3.2. The case of moving the error microphones

We verify the effectiveness of the ANC systems using the multi-channel perturbation method in the environment that the secondary paths always change. Two error microphones are moved like **Fig. 8**. **Figure 8** shows two error microphones moved like the point $\mathrm{A} \rightarrow \mathrm{B} \rightarrow \mathrm{A} \rightarrow \mathrm{C} \rightarrow \mathrm{A} \rightarrow \mathrm{B} \cdots$. The interval of the two error microphones is fixed and the center between the two error microphones is moved to each point. Moreover, in the points A, B and C, the system operates without moving the two error microphones for $20 \sim 30$ seconds. **Figure 9** shows error signals of the ANC system to multi-sinusoidal waves obtained in error microphone 1. In **Fig. 9**, (a) is the case that the ANC system is stopped and (b) is the case that the ANC system is executed. It can be seen from **Fig. 9** that the ANC system can operate stably in the environment that secondary paths always change. Therefore, this system has a great advantage that error microphones can be freely moved while the ANC system controls noise.

4. CONCLUSION

In this paper, we have verified the effectiveness of the multi-channel ANC systems using the perturbation method in actual systems. We have demonstrated that the ANC systems using the multi-channel perturbation method have an advantage which can operate stably if secondary paths change. Also, we have demonstrated that the ANC systems using the multi-channel perturbation method have a grate advantage that error microphones can be freely moved while the ANC system controls noise.

5. REFERENCES

[1] T. Mori, Y. Kajikawa and Y. Nomura, “Frequency domain active noise control systems using the time difference simultabeous perturbation method,” IEICE Trans. Fundamentals, vol.E86-A, no.4, pp.946–949, Apr. 2003.

[2] Y. Kajikawa and Y. Nomura, “Active noise control without a secondary path model by using a frequency-domain simultaneous perturbation method with variable perturbation,” Proc. of the 2003 IEEE International Conference on Acoustic, Speech, and Signal Processing, Hong Kong, China, Apr. 2003.

[3] Y. Kajikawa and Y. Nomura, “Frequency domain active noise control system without a secondary path model via perturbation method,” IEICE Trans. on Fundamentals, vol.E84-A, no.12, pp.3090–3098, Dec. 2001.